CCUS: 4193606

Corrosion Control in Carbon Storage by Injection of Sodium Formate Solution

Doguhan Barlas Sevindik[1], Oluwafemi Precious Oyenowo[1], Ryosuke Okuno[1], Muhammad Farooq Zia[2], Bo Zhang[2],

1. Hildebrand Department of Petroleum and Geosystems Engineering, The University of Texas at Austin, Austin, TX, United States.
2. Department of Civil and Environmental Engineering, University of Alberta, Edmonton, AB, Canada.

Abstract

Carbon dioxide (CO_2) leakage poses a significant risk to carbon storage in saline aquifers. Due to buoyant forces, CO_2 in resident brine can migrate into overlying formations through faults, fractures, or existing wells. Existing wells are particularly vulnerable to leakage because CO_2 creates an acidic environment when dissolved in brine, potentially leading to corrosion, as recently observed in the Illinois Basin Decatur Project (IBDP). This research investigates the injection of sodium formate solution as a strategy for corrosion control. Formate salts (e.g., sodium and potassium formates) have been widely used in oil fields as corrosion control agents and densifiers, and they can also serve as carbon carriers in carbon capture and storage (CCS) when produced from captured CO_2.

We conducted reactive transport simulations of CO_2 and formate solution injections using a well-characterized IBDP geologic model. This model has lateral dimensions of 15 × 15 km² and a thickness exceeding 1 km. It includes all essential geological formations, including Mt. Simon, as well as existing injectors and monitoring wells. We performed several cases of sodium formate solution injection with varying cumulative amounts of injected formate and compared them to the baseline case of CO_2 injection without corrosion control.

The simulation cases involving a pre-flush with sodium formate solutions indicated that formate, acting as a corrosion control agent, could spread effectively through the injected CO_2. A larger amount of formate injection resulted in a more extensive buffer zone and a more significant pH buffering effect. However, the monitoring well is located 730 meters away from the CO_2 injector, and the formate-based buffer zone did not extend to the monitoring well in the scenarios examined in this research. To mitigate pH reduction near the injector, formate does not need to spread far; a small amount of injection is sufficient to maintain the pH between 4.5 and 6.1 (the original pH). The injection of sodium formate, which raises

the pH from 3.2 (without formate) to 4.5 (with formate), is expected to significantly reduce the corrosion risk for 13 chrome steel pipes.

A comparison between pre-flush and post-flush methods of sodium formate application suggests that the pre-flush method is more effective for distributing the injected formate. In contrast, the post-flush method efficiently contains the injection well (such as CO_2 injectors and monitoring wells) using a smaller volume of sodium formate solution.

1. Introduction

The Intergovernmental Panel on Climate Change (IPCC) has highlighted the urgent need for innovative technologies to suppress the increasing levels of greenhouse gases in the atmosphere (IPCC, 2021). Among greenhouse gases, CO_2 contributes approximately 80% of annual emissions (Caesar et al., 2021; US EPA, 2024). It is crucial to reduce CO_2 emissions while still meeting global energy demands is crucial.

Carbon capture, utilization, and storage (CCUS) has emerged as a leading technology to mitigate CO_2 emissions (Dziejarski et al., 2023; Orr, 2018; Zhang et al., 2020). This process involves capturing CO_2 from point sources and securely storing it in suitable subsurface environments, such as depleted oil and gas reservoirs, hydrothermal reservoirs, and saline aquifers (Sevindik et al., 2023; Bachu, 2015).

Considering candidate environments for CO_2 storage, saline aquifers are well-studied subsurface environments that exhibit various CO_2 trapping mechanisms, including structural, solubility, capillary, and mineral trapping, when the right conditions are met (Izgec et al., 2008; Juanes et al., 2006; De Silva et al., 2015). Some of the largest commercial-scale CO_2 storage operations occur in saline aquifers. Notable examples include Quest (Bourne et al., 2014), Sleipner (Bachu and Gunter, 2004), and Snøhvit in Norway (Maldal and Tappel, 2004). These operations store more than 2 million tonnes (Mt) of CO_2 annually.

More recently, the Illinois Basin Decatur Project (IBDP) was initiated and has completed two phases of CO_2 injection (Finley, 2014; Couëslan et al., 2014). In the first phase, 1 Mt of supercritical CO_2 was injected. The second phase had a target amount of 5 Mt for injection into the Mt. Simon formation, a saline aquifer in the Midwest USA, Illinois.

CO_2 storage in deep subsurface reservoirs carries the risk of leakage, which can occur through various mechanisms. These mechanisms include CO_2 leakage due to inadequate sealing of the overlying formations or the presence of hydraulic pathways between the reservoir and the surface (Tokel et al., 2023; Szizybalski et al., 2023), geomechanical issues related to well integrity and induced seismicity (Dempsey et al., 2014; Verdon et al., 2011; Bai et al., 2015), and leakage associated with the acidification of the reservoir brine by dissolved CO_2.

When CO_2 dissolves in brine, it forms CO_2(aq) and carbonic acid. The dissociation of this carbonic acid primarily contributes to lowering pH levels (Liu et al. 2011), thereby creating an acidic brine that promotes corrosion and forms leakage pathways from the wells (Druhan et al., 2014; Xu et al., 2011). For example, at the Frio CCS project, 1600 tonnes of CO_2 were injected into the Frio Formation—a 1500-meter-deep sandstone saline aquifer (Kharaka et al., 2006). Monitoring wells at this location recorded significant pH reductions following the breakthrough of CO_2. Geochemical modeling studies suggest that this could lead to potential leakage of CO_2 and brine through the caprock and cement around the wells (Kharaka et al., 2006; Ilgen and Cygan, 2016).

The US Environmental Protection Agency (EPA) recently published a notice of alleged violations in the IBDP sequestration project due to CO_2 migration into unauthorized zones. The operator reported that the CO_2 migration resulted from tubing corrosion in a monitoring well (US EPA, 2024), underscoring the need to consider the effect of pH on wells (e.g., CO_2 injectors and monitoring wells) in CCS projects. Although CO_2 injectors may be surrounded by less brine during the injection period, capillary/gravity/thermodynamic equilibrium processes will cause water imbibition to increase water saturation near the injectors after CO_2 injection. Therefore, corrosion control is essential not only for monitoring wells but also for CO_2 injectors.

In this study, we aim to investigate the effectiveness of sodium formate as a corrosion control substance in the near-wellbore region. Formate species, such as sodium and potassium formates, have

traditionally been used as densifiers and corrosion inhibitors due to their favorable health, safety, and environmental (HSE) profiles. They are also studied as carbon carriers for CCS/CCUS (Mirzaei-Paiaman et al., 2024; Oyenowo et al., 2023; Wang et al., 2023; Okuno, 2022; Mirzaei-Paiaman et al., 2025) because formate can be produced from captured CO_2 in various ways. If electrochemical reduction (ECR) of CO_2 is performed at scale, formate species can be generated using renewable energy sources, such as solar, wind, and geothermal energy, for CCS/CCUS. The CO_2 ECR technology currently has a Technology Readiness Level (TRL) of 6 (CORDIS, 2022).

Using aqueous formate solutions offers several advantages over traditional CO_2 injection operations. It can lower operational and monitoring expenses and allow for the effective use of rock pore space for carbon storage when highly concentrated formate solutions are injected (Oyenowo et al. 2021, 2023). Recent efforts have focused on implementing aqueous formate solutions as alternative carbon carriers (Mirzaei-Paiaman et al., 2024; Oyenowo et al., 2023; Wang et al., 2023; Okuno, 2022; Mirzaei-Paiaman et al., 2025; Breunig et al., 2023) and as wettability alteration agents for enhanced oil recovery (Baghishov et al., 2022; Oyenowo et al., 2024).

In this simulation study, we modeled the injection of aqueous formate solutions using a numerical simulation model for the IBDP injection site, where corrosion is a known problem, according to a recent US EPA notice. Although the current concern at IBDP involves the corrosion of a monitoring well, these wells are typically not designed for fluid injection to control corrosion. Therefore, this study focused on using the CO_2 injector at IBDP CCS2 to explore scenarios of well treatment with sodium formate solutions.

First, we describe the IBDP injection site and the geological model previously developed by Greenberg (2021). We then detail the mechanisms of aqueous formate reactions and the injection scenarios. Finally, we present the simulation results, which show the impacts on the reservoir and near-wellbore pH levels, along with potential recommendations.

2. Numerical simulation model and scenarios

This section describes the geological setting of the injection area, the numerical model, the chemical reactions considered, and the formate injection strategies.

2.1 Geology of the IBDP CO_2 injection site

The target and sealing zones at the IBDP site primarily consist of Paleozoic sedimentary rocks from the Middle Cambrian period and a Precambrian basement composed of igneous and highly fractured rhyolites (Collinson, 1988; Berger, 2019). The main targeted zone for CO_2 injection is the Mt. Simon sandstone, a saline aquifer extending from Illinois to western Kentucky. This aquifer is approximately 500 meters thick at the injection site, where the target injection depth is around 7,000 feet (Greenberg, 2021).

This zone is divided into three subzones: upper, middle, and lower (Dewers et al., 2014; Freiburg et al., 2020). The lower Mt. Simon subzone has the best reservoir quality, with an average porosity of 25% and permeability values as high as 1066 mD. This subzone consists of cross-bedded subarkose sandstone and conglomerates with clay intrusions. The middle subzone primarily contains quartz arenites formed in aeolian and braided river environments and features significant quartz cementation (Freiburg et al., 2014). This cementation has resulted in poorer reservoir quality, with average porosity and permeability values of 12% and 44 mD, respectively.

The upper subzone consists of sandy and silty shales, capped by the primary sealing formation, the Eau Claire Formation (Palkovic, 2015). The Eau Claire Formation includes siltstones and shales, with some carbonate-bearing rocks such as mudstones and dolomites in its upper section. Between the igneous Precambrian basement and the lower section of the Mt. Simon formation lies a thin, unconformably positioned sedimentary formation known as the Argenta Formation. This formation comprises clay-rich conglomerates and sandstones (Freiburg et al., 2015). A schematic of the stratigraphic column of the formations can be observed in Figure 1.

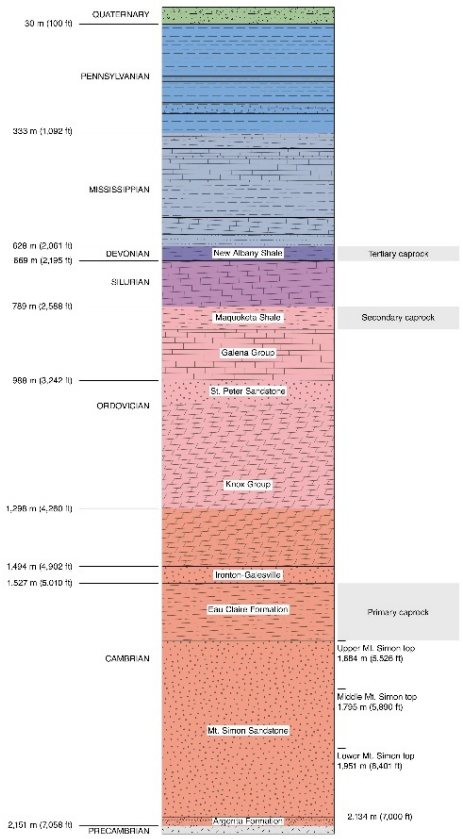

Figure 1. Stratigraphic column of the IBDP injection site (ISGS – IBDP, 2021)

2.2 Simulation model

The construction of the IBDP conceptual geological model and the dynamic reservoir model used in this research is based on the descriptions presented in Greenberg (2021). The reservoir model, illustrated in Figure 2, includes geological formations such as the Eau Claire, multiple zones of the Mt. Simon Formation, the Argenta Formation, and the Precambrian Basement. To facilitate the targeted injection activities within the lower Mt. Simon subzone, additional vertical grid refinement has been applied, yielding a total of 110 grid layers in the vertical (z) direction.

The grid block refinement is more detailed near the wells and progressively coarser toward the boundaries, resulting in approximately 1,732,500 active grid blocks in the model. This coarser grid distribution away from the wells, combined with large volume modifiers at the lateral boundaries of the model (excluding the top and bottom), creates a constant pressure boundary that simulates the surrounding aquifer. All operational wells, including both injection and verification wells, are incorporated into the reservoir model. The distributions of porosity and permeability within the model are depicted in Figure 2.

For the relative permeability and capillary pressure of the CO_2-water system, three distinct sets of properties have been incorporated into the reservoir model, following the recommendations of Mehnert et al. (2019). These relative permeability curves are categorized based on rock quality—high, intermediate, and low—resulting in varied sets of relative permeability and capillary pressures, in line with the guidelines established by Mehnert et al. (2019) and Greenberg (2021). The reservoir model was utilized to simulate CO_2 transport and to investigate the effects of formate injection on pH levels. A coupled flow and reactive model was developed using the compositional reservoir simulator CMG-GEM (as outlined in the CMG-GEM User Manual, 2023).

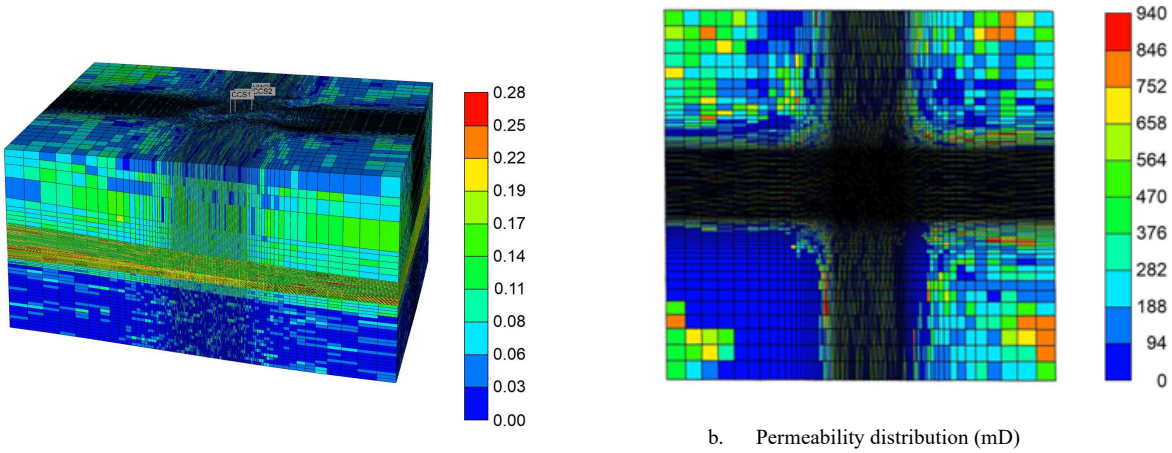

a. Porosity distribution

b. Permeability distribution (mD)

Figure 2. Porosity and permeability distributions were used in the simulation study.

2.3 Properties of reservoir and injected brines

For modeling the aqueous phase, the composition of the Mt. Simon formation brine was obtained from Locke II et al. (2013). This brine was primarily composed of sodium chloride; thus, the simulation in this study utilized a NaCl brine with a salinity of 170,000 ppm.

To account for the chemical reactions in the CO_2-brine system with Na^+ and Cl^-, the following reactions were implemented (Equations (1) to (4)) based on the kinetic data provided in the Wolery geochemical database (Wolery and Jarek, 2003).

$$CO_2 + H_2O = H^+ + OH^- \quad (1)$$

$$H^+ + OH^- = H_2O \quad (2)$$

$$CO_3^{2-} + H^+ = HCO_3^- \quad (3)$$

$$NaCl = Cl^- + Na^+ \quad (4)$$

For the injection of the sodium formate solution, additional reactions involving the association and dissociation of sodium formate and formic acid were introduced to the model accordingly. Below, the formate ion is denoted as FM^-. The kinetic parameters for equations 5 and 6 were taken from Felmy et al. (1984) and Shock and Koretsky (1995), respectively.

	$\log_{10} K_{25\,°C}$	$\Delta H_{25\,°C}$ (kj/mol)	
$H^+ + FM^- = H(FM)$	3.745	0.167	(5)
$Na^+ + FM^- = Na(FM)$	0.117	-1.325	(6)

The viscosity of the gas phase was calculated using the correlation developed by Jossi, Stiel, and Thodos (Reid et al., 1987). The gas density was determined using the Peng-Robinson equation of state (Peng and Robinson, 1978). For the aqueous phase, the density and viscosity were calculated using the Rowe and Chou correlation (1970) and the method of Kestin et al. (1981), respectively. The density and solubility data for sodium formate were sourced from Oyenowo et al. (2023), while the pH of the aqueous solution was obtained from Wang et al. (2025). Table 1 presents the density of the formate solution and the pH values corresponding to various concentrations of the formate ion in brine at 25°C. As formate is the conjugate base of formic acid, an increase in the concentration of sodium formate results in a more basic aqueous solution.

Table 1. Density and pH of the formate solutions in brine at 25℃ (Oyenowo et al, 2023; Wang et al., 2025).

Formate concentration (% w/w)	Molar concentration (mol/l)	Density (kg/m^3)	pH
5.0	1.26	1136.0	7.63
15.0	4.50	1214.0	8.06
20.0	5.61	1262.5	8.29
29.6	9.00	1367.5	8.69

2.4 Injection scenarios

The CO_2 injection project was conducted in two phases from two wells, CCS1 and CCS2. The first phase began at the CCS1 well in November 2011, during which 1 Mt of CO_2 was injected over a period of three years. After this initial phase, there were no injections until the second phase commenced at the CCS2 well in April 2017. The injections from this well continued until it stopped recently, targeting a cumulative total of 5 Mt of CO_2.

Various quantities and concentrations of sodium formate were injected to evaluate the effects of sodium formate injection on pH levels near and far from the CCS2 well. Four scenarios involving sodium formate injection were compared against a base case of CO_2 injection without formate treatment (as shown in Table 2). A higher concentration of 15 wt% was chosen, as it remains well below the solubility limit for sodium formate (Oyenowo et al., 2023).

In all injection strategies (see Table 2), it was assumed that a sodium formate solution would be injected at a constant rate for one year before CO_2 injection began from the CCS2 well. This approach resulted in varying cumulative amounts of sodium formate and water being injected into the formation. The subsequent CO_2 injection promoted the convective spreading of the corrosion inhibitor, the formate anion.

Table 2. Four scenarios of sodium formate injection for well treatment of CO_2 injector in the IBDP model. The solution pH is 7.63 for 5.0 wt% formate and 8.06 for 15.0 wt% formate, as shown in Table 1.

Scenarios	Injection rate bbl/D	Formate concentration		Formate injected Million moles	Incremental pH in well grid blocks
		wt%	mol/L		
a	500	5.0	1.26	36.56	1.27
b	500	15.0	4.50	117.52	1.43
c	4,000	5.0	1.26	292.50	1.45
d	4,000	15.0	4.50	940.17	1.59

3. Results and discussions

This section presents the simulation results for the IBDP site, focusing on the migration of the CO_2 plume and the changes in pH levels, both with and without formate injection. It encompasses the total cumulative CO_2 injection for the first two phases of the project from the CCS1 and CCS2 wells, respectively.

3.1 CO_2 injection without corrosion control by formate

As previously described, the base case simulated CO_2 injection in two phases from wells CCS1 (1 Mt) and CCS2 (5 Mt). Figure 3 illustrates the behavior of the CO_2 plume and the changes in pH within the reservoir at one year, three years, and five years after the beginning of CO_2 injection, as well as at the end of the injection period from CCS2. The area near the injector shows a significantly low pH value of 3.2.

The results indicate that the pH plume contains the CO_2 plume because the mixing of CO_2 and water leads to acidic pH conditions near the CO_2 front. Consequently, the distance between the CO_2 and pH fronts is likely influenced by the inherent heterogeneity of the reservoir and the numerical discretization used in the simulation. In this case, the simulated distance between the CO_2 and pH fronts was found to be

quite substantial. The corrosion observed in the monitoring well at CCS2 in IBDP emphasizes the importance of accurately estimating the migration of the pH plume.

Figure 4 depicts the evolution of pH at the monitoring well during the base case simulation. When the pH plume reached the monitoring well, the pH dropped from an initial value of 6.1 to 4.6, indicating a reduction of 1.5 in pH. The pH can be even lower within the CO_2 plume, as shown in Figure 3. However, monitoring wells are typically not drilled for fluid injection, as is the case with the IBDP; for instance, the permeability of the perforation interval must be assessed for injection wells. Therefore, this paper primarily focuses on injecting the sodium formate solution from the CO_2 injector.

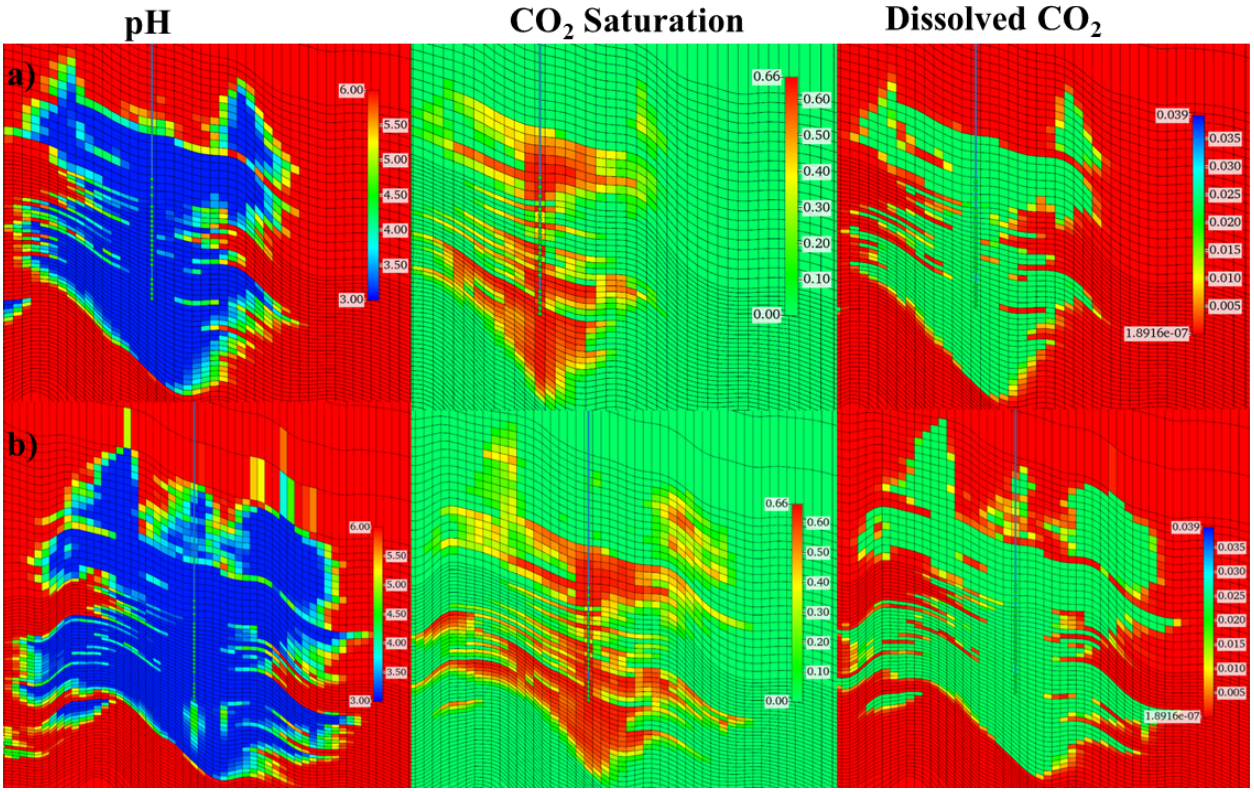

Figure 3. pH evolution, CO_2-gas plume, and dissolved CO_2 around the CCS2 well in the reservoir (a) after 3 years and (b) at the end of the CO_2 injection.

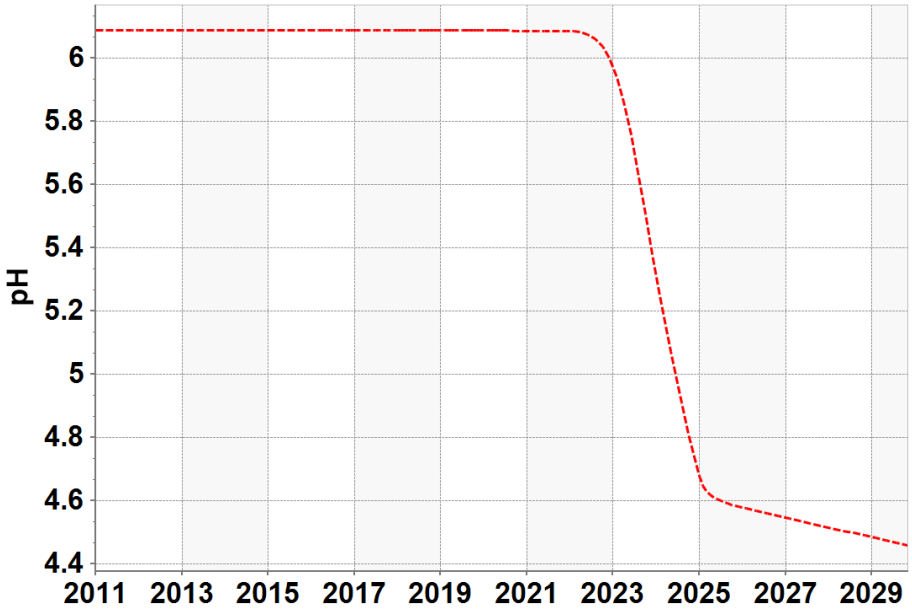

Figure 4. pH history in the gridblock with the monitoring well without injecting a sodium formate solution.

3.2 Sodium formate injection prior to CO_2 injection

Figure 5 illustrates the pH changes in the near-wellbore region of the CCS2 well following three years of CO_2 injection, which occurred four years after the injection of formate. In contrast to Figure 3, Figure 5 demonstrates that the formate solution served as an effective pH buffer in the near-wellbore area (shown in green). The green region expanded as more sodium formate was injected, with the order of effectiveness being Cases a < b < c < d.

As CO_2 is injected into the reservoir, it lowers the pH due to the formation of carbonic acid (see Equation 1). The prior injection of sodium formate acts as a pre-flush for the well, allowing formate ions in the near-wellbore region to bond with protons, as described in Equation 5. This reaction decreases the concentration of hydrogen ions, thereby mitigating the pH reduction caused by CO_2 injection.

Results from Cases a to d indicate that the pre-flush with sodium formate solutions can spread the corrosion control agent, formate ions, during subsequent CO_2 injection. For instance, in Case a, formate fronts extended approximately 180 meters from the injector after 5 Mt of CO_2 were injected over 8 years, while in Case d, they reached 400 meters. However, in the IBDP case studied, the monitoring well experiencing corrosion was located 730 meters away from the injector and was not influenced by the formate (refer to Figure 4).

If sodium formate injection is conducted solely to suppress pH reduction near the injector, a small amount of injection (less than that used in Case a) will be sufficient to maintain the pH between 4.5 and 6.1 (the original pH), as illustrated in Figure 5. The sodium formate injection, which raises the pH from 3.2 (without formate) to 4.5 (with formate), is expected to significantly reduce the risk of corrosion of 13 chrome steel pipes, as noted by Rincon et al. (2005).

Figure 6 presents the pH profiles for Cases a to d after 8 years of CO_2 injection, during which 5 Mt of CO_2 was injected. Despite the considerable CO_2 throughput, all cases demonstrate a suppression of pH drop near the injector due to the pre-flush by a sodium formate solution—however, a larger amount of injected formate results in a more substantial pH buffering effect. A comparison between Figures 5 and 6 shows that CO_2 reduced the green region more significantly in Case a than in Case d.

Figure 7 illustrates the change in pH (the pH value from the formate injection cases minus the pH value from the CO_2 injection without formate) for the wellbore intersecting grid blocks based on the amount of sodium formate injected. As more sodium formate is injected, the pH in the wellbore grid blocks increases compared to the baseline case of CO_2 injection without sodium formate.

The comparisons between Cases a and b, as well as Cases c and d, demonstrate that the 15-wt% formate injection was more effective than the 5-wt% formate injection in mitigating the pH drop caused by CO_2 injection. Furthermore, Cases b and c produced similar changes in pH, indicating that Case b was more efficient than Case c. Generally, a smaller amount of pre-flush is preferred in CCS since the primary objective is to inject CO_2.

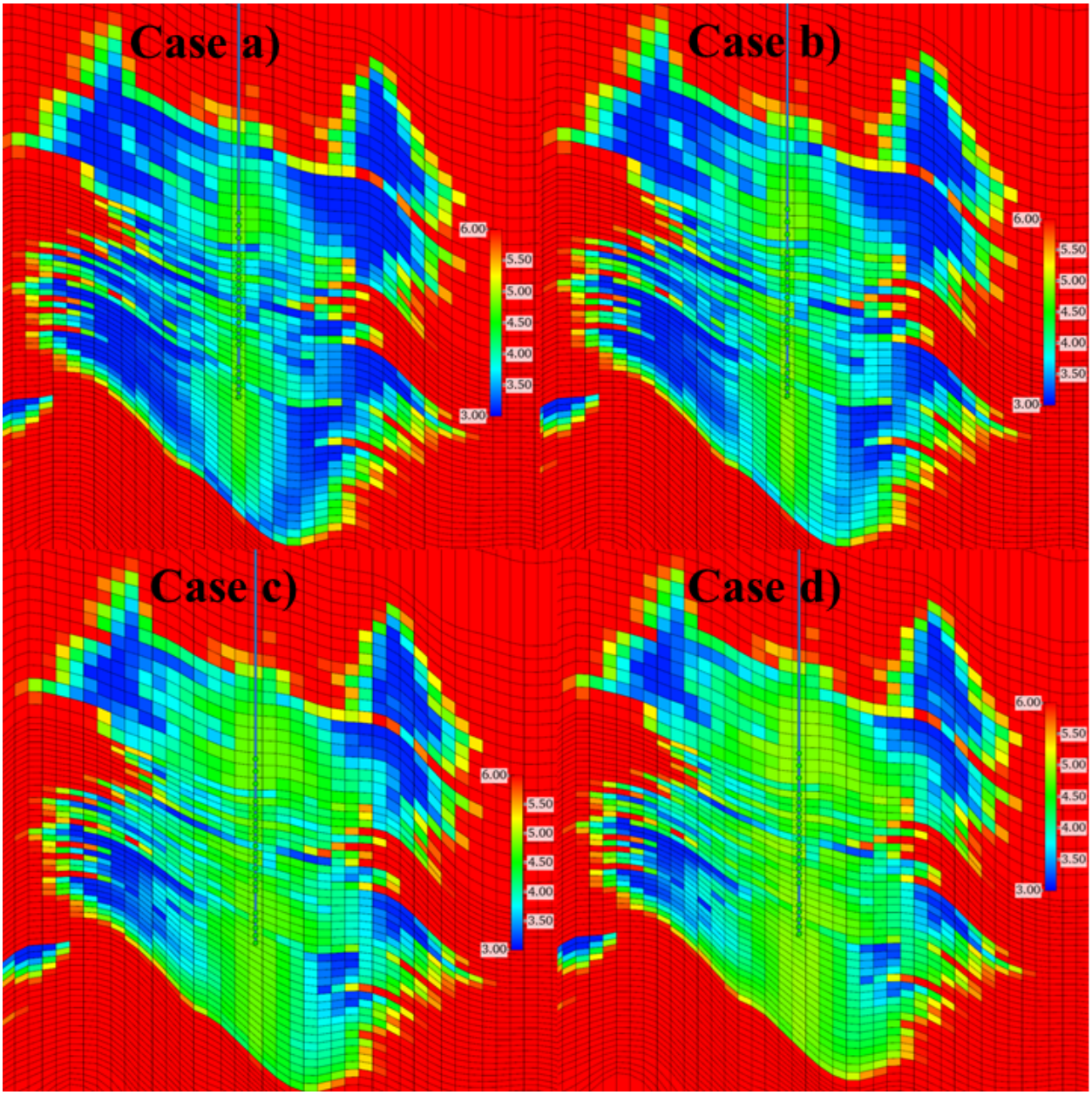

Figure 5. pH evolution near the CCS2 well after 3 years of CO_2 injection.

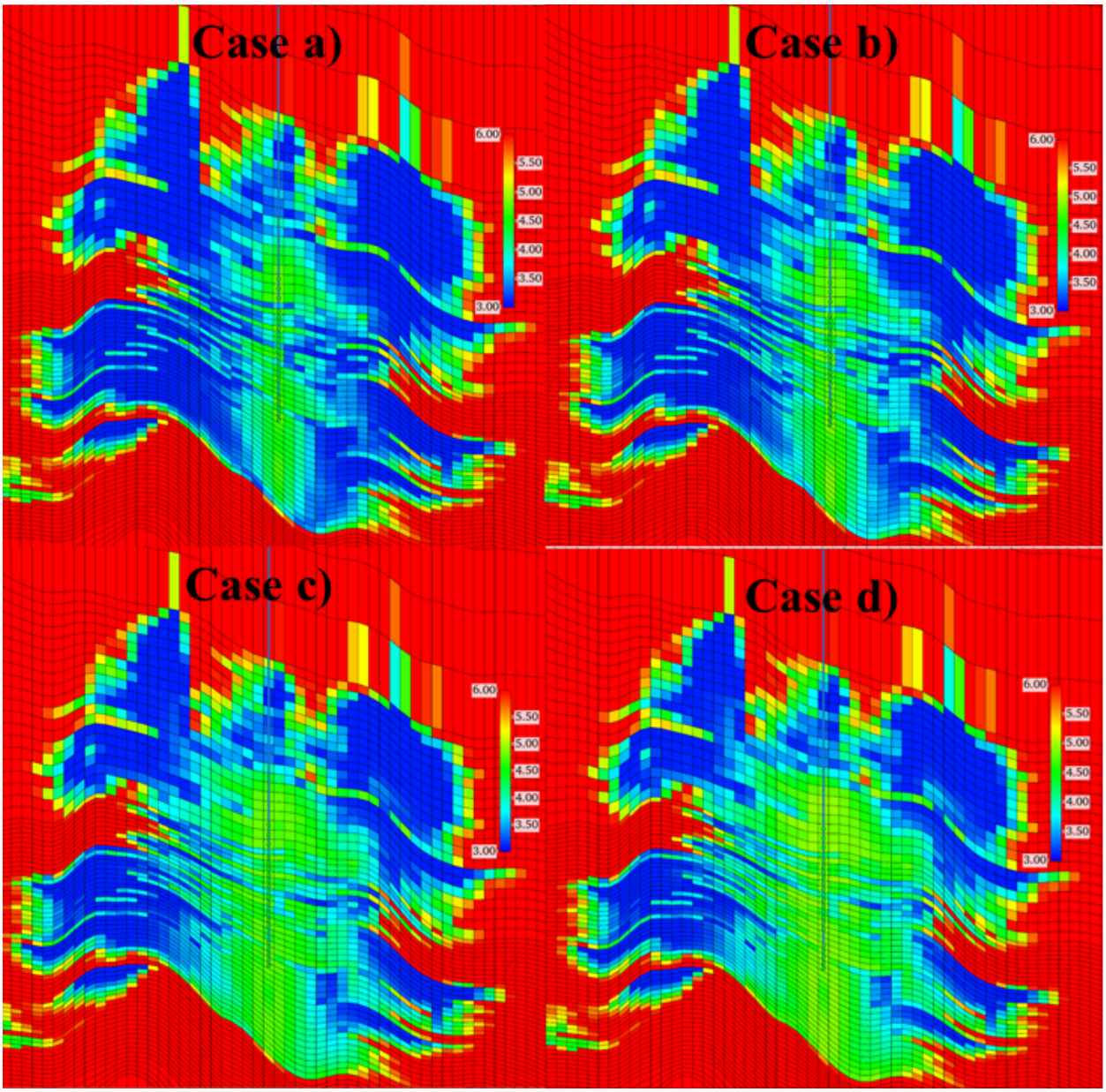

Figure 6. pH evolution at the end of the 5 million tons of CO_2 injection around the CCS2 (8 years of CO_2 injection).

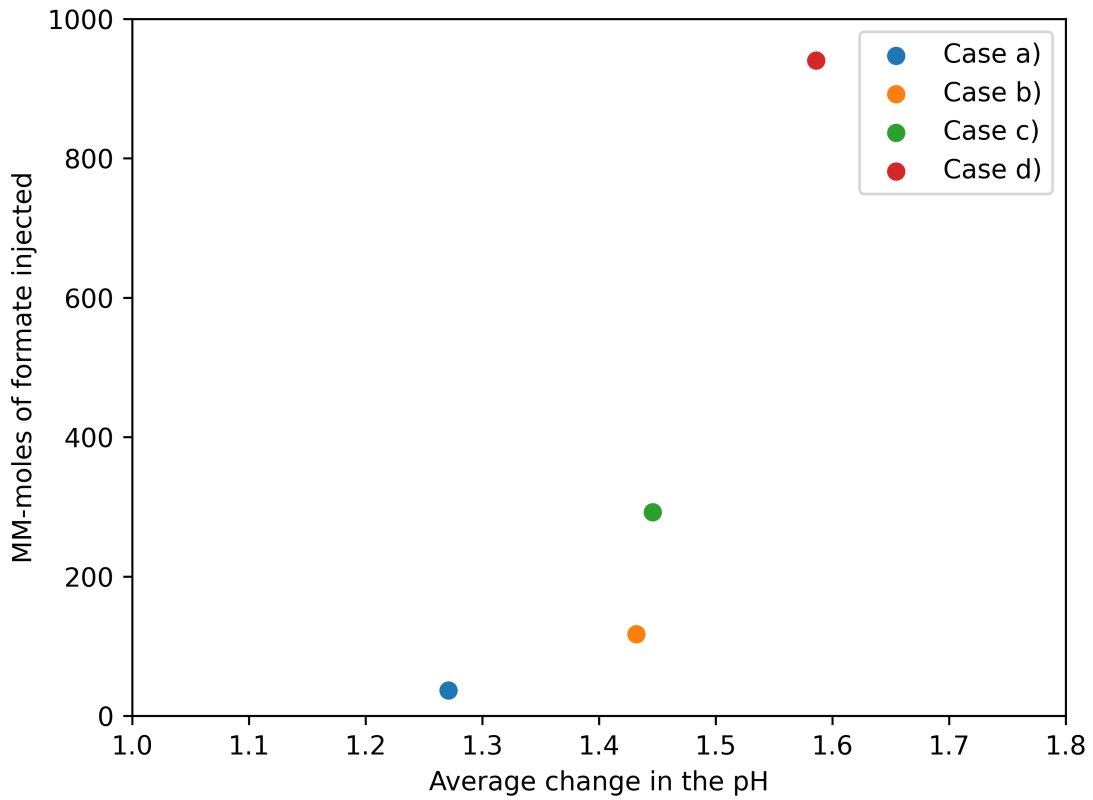

Figure 7. Simulated pH changes in well-bore gridblocks for Cases a – d with respect to the amount of formate injected at the end of 5 Mt CO_2 injection (8 years after the start of CO_2 injection). The pH change is defined as "the pH value with sodium formate injection less the pH value without sodium formate injection."

3.3 Post-flush compared to pre-flush

In addition to pre-flushing the well with an aqueous formate solution, post-flushing was also conducted to evaluate its advantages over pre-flushing. The purpose of simulating the post-flush was to determine whether formate injection could be used in a remedial manner, specifically to see if the pH around the well could be restored after CO_2 injection has created an acidic environment. The main difference between post-flush and pre-flush is that the formate cannot be spread by the CO_2 injection, unlike in pre-flushing, as illustrated in Figures 5 and 6.

For this test, Case a was used, but the aqueous formate solution was injected for one year immediately after completing the CO_2 injection. Figure 8 illustrates the pH evolution in the near-wellbore region of the CCS2 well after 1 year and 3 years from the formate injection.

The comparison between the post-flush and pre-flush of sodium formate is illustrated in Figures 6a and 8b, which both use the same quantity of sodium formate injected. As previously mentioned, the pH buffer zone in Figure 6a extends approximately 180 meters, whereas in Figure 8b, it spans around 60 meters. The pre-flush method is advantageous for distributing the injected formate, which serves as a corrosion control material. In contrast, the post-flush method is effective for efficiently containing the injection well (such as CO_2 injectors and monitoring wells) using a smaller volume of sodium formate solution.

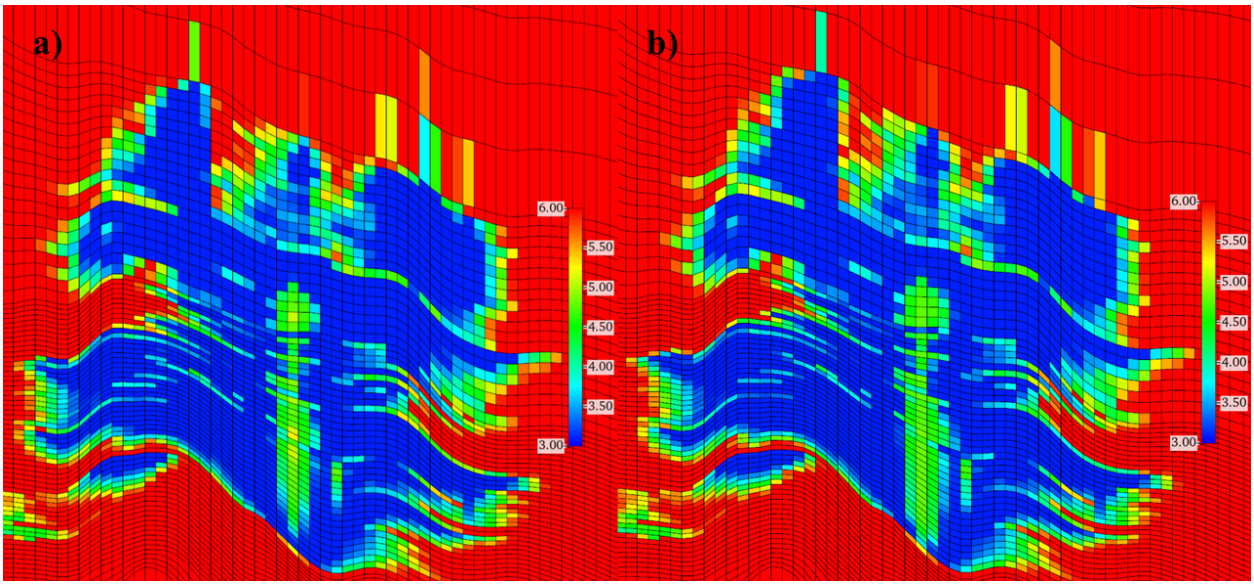

Figure 8. pH profiles around CCS2 after one year (a) and three years (b) of the completion of sodium formate post-flush. A comparison between parts a and b shows that the formate did not spread for two years in the post-flush scenario.

4. Conclusions

This paper presents a numerical simulation study on the injection of sodium formate solutions for corrosion control using the IBDP model. The IBDP model was utilized in part due to the recent discovery of CO_2 migration into unauthorized zones through a monitoring well, emphasizing the need for effective corrosion control in Carbon Capture and Storage (CCS). Sodium formate was selected as a corrosion control agent because it has been widely used in oil fields and can function as a carbon carrier in CCS when generated from captured CO_2. The main conclusions are as follows:

1. The simulation demonstrated that the pH plume was significantly greater than the CO_2 plume due to the mixing and spreading of carbon species during the CO_2 injection simulation with a heterogeneous IBDP model. When the pH plume reached the monitoring well of concern, a rapid drop in pH was observed, decreasing from an initial value of 6.1 to 4.6, with further declines as the CO_2 plume expanded.

2. Simulation cases involving a pre-flush with sodium formate solutions in the CCS-2 well showed that formate, serving as a corrosion control agent, could effectively spread through the injected CO_2. A larger amount of formate injection resulted in a more extensive buffer zone and a more significant pH buffering effect. However, the monitoring well in question is located 730 meters away from the CO_2 injector, and the formate-based buffer zone did not reach the monitoring well in the scenarios examined in this research.

3. To mitigate pH reduction near the injector, it is not necessary for formate to spread away from the injector; a small amount of injection (less than that used in Case a) is sufficient to maintain the pH between 4.5 and 6.1 (the original pH). The injection of sodium formate, which raises the pH from 3.2 (without formate) to 4.5 (with formate), is expected to significantly reduce the corrosion risk for 13 chrome steel pipes, as indicated by Rincon et al. (2005).

4. A comparison between pre-flush and post-flush methods of sodium formate application suggests that the pre-flush method is more effective for distributing the injected formate. Conversely, the post-flush method efficiently contains the injection well (such as CO_2 injectors and monitoring wells) using a smaller volume of sodium formate solution.

Acknowledgements
We thank the sponsors of the Energi Simulation Industrial Affiliate Program on Carbon Utilization and Storage (ES Carbon UT) at the Center for Subsurface Energy and the Environment at the University of Texas at Austin. Ryosuke Okuno holds the Pioneer Corporation Faculty Fellowship in the Hildebrand Department of Petroleum and Geosystems Engineering at the University of Texas at Austin.

References

Bachu, S. 2015. Review of CO_2 storage efficiency in deep saline aquifers. *International Journal of Greenhouse Gas Control* **40**: 188-202. https://doi.org/10.1016/j.ijggc.2015.01.007.

Baghishov, I., Abeykoon, G., Wang, M. et al. 2022. A mechanistic comparison of formate, acetate, and glycine as wettability modifiers for carbonate and shale formations. *Colloids and Surfaces A: Physicochemical and Engineering Aspects* **652**: 129849. https://doi.org/10.1016/j.colsurfa.2022.129849.

Bai, M., Sun, J., Song, K. et al. 2015. Evaluation of mechanical well integrity during CO_2 underground storage. *Environmental Earth Sciences* **73** (11): 6815-6825. https://doi.org/10.1007/s12665-015-4157-5.

Berger, P., Yoksoulian, L., Freiburg, J. et al. 2019. Carbon sequestration at the Illinois Basin-Decatur Project: experimental results and geochemical simulations of storage. *Environmental Earth Sciences* **78** (22): 646. https://doi.org/10.1007/s12665-019-8659-4.

Bourne, S., Crouch, S., and Smith, M. 2014. A risk-based framework for measurement, monitoring and verification of the Quest CCS Project, Alberta, Canada. *International Journal of Greenhouse Gas Control* **26**: 109-126. https://doi.org/10.1016/j.ijggc.2014.04.026.

Breunig, H., Rosner, F., Lim, T. et al. 2023. Emerging concepts in intermediate carbon dioxide emplacement to support carbon dioxide removal. *Energy & Environmental Science* **16** (5): 1821-1837. https://doi.org/10.1039/d2ee03623a.

Caesar, L., McCarthy, G., Thornalley, D. et al. 2021. Current Atlantic Meridional Overturning Circulation weakest in last millennium. *Nature Geoscience* **14** (3): 118-120. https://doi.org/10.1038/s41561-021-00699-z.

Collinson, C., Sargent, M.L., Jennings, J.R. 1988. Illinois Basin region. *Sedimentary Cover—North American Craton: U.S*. Sloss. L.L., 383–426: Geological Society of America, Inc.

Computer Modeling Group (CMG), GEM User Manual, 2023

Couëslan, M., Butsch, R., Will, R. et al. 2014. Integrated reservoir monitoring at the Illinois Basin – Decatur Project. *Energy Procedia* **63**: 2836-2847. https://doi.org/10.1016/j.egypro.2014.11.306.

De Silva, G., Ranjith, P., and Perera, M. 2015. Geochemical aspects of CO_2 sequestration in deep saline aquifers: A review. *Fuel* **155**: 128-143. https://doi.org/10.1016/j.fuel.2015.03.045.

Dempsey, D., Kelkar, S., Pawar, R. et al. 2014. Modeling caprock bending stresses and their potential for induced seismicity during CO_2 injection. *International Journal of Greenhouse Gas Control* **22**: 223-236. https://doi.org/10.1016/j.ijggc.2014.01.005.

Dewers, T., Newell, P., Broome, S. et al. 2014. Geomechanical behavior of Cambrian Mount Simon Sandstone reservoir lithofacies, Iowa Shelf, USA. *International Journal of Greenhouse Gas Control* **21**: 33-48. https://doi.org/10.1016/j.ijggc.2013.11.010.

Druhan, J., Vialle, S., Maher, K. et al. 2014. A reactive transport model for geochemical mitigation of CO_2 leaking into a confined aquifer. *Energy Procedia* **63**: 4620-4629. https://doi.org/10.1016/j.egypro.2014.11.495.

Dziejarski, B., Krzyżyńska, R., and Andersson, K. 2023. Current status of carbon capture, utilization, and storage technologies in the global economy: A survey of technical assessment. *Fuel* **342**: 127776. https://doi.org/10.1016/j.fuel.2023.127776.

European Commission CORDIS. 2022. Oxalic acid from CO_2 using electrochemistry at demonstratioN scale. https://doi.org/10.3030/767798.

Felmy, A., Girvin, D., and Jenne, E. 1984. MINTEQ—A Computer Program for Calculating Aqueous Geochemical Equilibria: February 1984. National Technical Information Service.

Finley, R. 2014. An overview of the Illinois Basin – Decatur Project. *Greenhouse Gases: Science and Technology* **4** (5): 571-579. https://doi.org/10.1002/ghg.1433.

Freiburg J. T., Morse D. G., Leetaru H. E. et al. 2014. A Depositional and Diagenetic Characterization of the Mt. Simon Sandstone at the Illinois Basin–Decatur Project Carbon Capture and Storage Site, Decatur, Illinois, USA. Circular 583, Ill. State Geol. Surv., Champaign

Freiburg, J., Leetaru, H., & Monson, C. 2015. The Argenta Formation; a newly recognized Cambrian stratigraphic unit in the Illinois Basin. Abstracts with Programs - Geological Society of America, Vol. 47(no. 5), p.86

Freiburg, J., McBride, J., Malone, D. et al. 2020. Petrology, geochronology, and geophysical characterization of Mesoproterozoic rocks in central Illinois, USA. *Geoscience Frontiers* **11** (2): 581-596. https://doi.org/10.1016/j.gsf.2019.07.004.

Greenberg, S.E. 2021. Illinois Basin – Decatur Project. An Assessment of Geological Carbon Sequestration Options in the Illinois Basin: Phase III. Final Report to the United States Department of Energy, Contract: DE-FC26-05NT42588, 426p.

Greenberg, S.E. 2021. Illinois State Geological Survey (ISGS), Illinois Basin - Decatur Project (IBDP) Geological Models, July 7, 2021. Midwest Geological Sequestration Consortium (MGSC) Phase III Data Sets. DOE Cooperative Agreement No. DE-FC26-05NT42588. United States. https://doi.org/10.18141/1854141

Ilgen, A. and Cygan, R. 2016. Mineral dissolution and precipitation during CO_2 injection at the Frio-I Brine Pilot: Geochemical modeling and uncertainty analysis. *International Journal of Greenhouse Gas Control* **44**: 166-174. https://doi.org/10.1016/j.ijggc.2015.11.022.

Illinois State Geological Survey (ISGS), Illinois Basin - Decatur Project (IBDP). 2021. Midwest Geological Sequestration Consortium (MGSC) Phase III Data Sets, DOE Cooperative Agreement No. DE-FC26-05NT42588.

Izgec, O., Demiral, B., Bertin, H. et al. 2008. CO_2 injection into saline carbonate aquifer formations I: laboratory investigation. *Transport in Porous Media* **72** (1): 1-24. https://doi.org/10.1007/s11242-007-9132-5.

Juanes, R., Spiteri, E., Orr, F. et al. 2006. Impact of relative permeability hysteresis on geological CO_2 storage. *Water Resources Research* **42** (12): https://doi.org/10.1029/2005wr004806.

Kestin, J., Khalifa, H., and Correia, R. 1981. Tables of the dynamic and kinematic viscosity of aqueous NaCl solutions in the temperature range 20–150 °C and the pressure range 0.1–35 MPa. *Journal of Physical and Chemical Reference Data* **10** (1): 71-88. https://doi.org/10.1063/1.555641.

Kharaka, Y., Cole, D., Thordsen, J. et al. 2006. Gas–water–rock interactions in sedimentary basins: CO_2 sequestration in the Frio Formation, Texas, USA. *Journal of Geochemical Exploration* **89**: 183-186. https://doi.org/10.1016/j.gexplo.2005.11.077.

Liu, F., Lu, P., Zhu, C. et al. 2011. Coupled reactive flow and transport modeling of CO_2 sequestration in the Mt. Simon sandstone formation, Midwest U.S.A. *International Journal of Greenhouse Gas Control* **5** (2): 294-307. https://doi.org/10.1016/j.ijggc.2010.08.008.

Locke Ii, R., Larssen, D., Salden, W. et al. 2013. Preinjection Reservoir Fluid Characterization at a CCS Demonstration Site: Illinois Basin – Decatur Project, USA. *Energy Procedia* **37**: 6424-6433. https://doi.org/10.1016/j.egypro.2013.06.572.

Maldal, T. and Tappel, I. 2004. CO_2 underground storage for Snøhvit gas field development. *Energy* **29**: 1403-1411. https://doi.org/10.1016/j.energy.2004.03.074.

Masson-Delmotte, V., P. Zhai, A. et al. 2021. *The Physical Science Basis. Contribution of Working Group I to the Sixth Assessment Report of the Intergovernmental Panel on Climate Change.* Cambridge University Press, Cambridge, United Kingdom and New York, NY, USA.

Mehnert, E., J.R. Damico, N.P. Grigsby, C.C. et al. 2019. Geologic carbon sequestration in the Illinois Basin: Numerical modeling to evaluate potential impacts: Illinois State Geological Survey, Circular 598, 71 p. State Geol. Surv., Champaign.

Mirzaei-Paiaman, A., Carrasco-Jaim, O., and Okuno, R. 2024. Techno-economic-environmental study of CO_2 and aqueous formate solution injection for geologic carbon storage and enhanced oil recovery. *International Journal of Greenhouse Gas Control* **138**: 104257. https://doi.org/10.1016/j.ijggc.2024.104257.

Mirzaei-Paiaman, A., Okuno, R., and Moscardelli, L. 2025. FAG: Alternating Injection of CO_2 and Aqueous Formate Solution for Maximizing Carbon Storage and Oil Recovery. Carbon Capture, Utilization, and Storage Conference. Houston, TX, USA, 3-5 March, 2025, CCUS: 4177285.

Okuno, R. 2022. Aqueous Formate Solution as a Novel Carbon Carrier for Geological Carbon Storage. Presented at EAGE Asia Pacific Workshop on CO_2 Geological Storage, August 2022. https://doi.org/10.3997/2214-4609.202275012

Orr, F. 2018. Carbon Capture, Utilization, and Storage: An Update. *SPE Journal* **23** (6): 2444-2455. https://doi.org/10.2118/194190-pa.

Oyenowo, O.P., Sheng, K., Abeykoon, G.A., and Okuno, R., A Case Study of Using Aqueous Formate Solution for Carbon Sequestration and Geological Storage, The GEOGULF 2021 Conference, October 27 – 29, 2021, Austin, Texas. GCAGS Transactions, Volume 71, pp. 203 – 215.

Oyenowo, O., Sheng, K., and Okuno, R. 2023. Simulation case studies of aqueous formate solution for geological carbon storage. *Fuel* **334**: 126643. https://doi.org/10.1016/j.fuel.2022.126643.

Oyenowo, O., Wang, H., Mirzaei-Paiaman, A. et al. 2024. Geochemical Impact of High-Concentration Formate Solution Injection on Rock Wettability for Enhanced Oil Recovery and Geologic Carbon Storage. *Energy & Fuels* **38** (7): 6138-6155. https://doi.org/10.1021/acs.energyfuels.3c05081.

Palkovic M.J. 2015. Depositional characterization of the Eau Claire Formation at the Illinois Basin – Decatur Project: Facies, mineralogy and geochemistry. MS Thesis. University of Illinois at Urbana-Champaign, Urbana, Illinois.

Peng, D. and Robinson, D. 1978. A New Two-Constant Equation of State. *Industrial & Engineering Chemistry Fundamentals* **15** (1): 59-64. https://doi.org/10.1021/i160057a011.

Reid, R.C., Prausnitz, J.M. and Poling, B.E. 1987. *The properties of gases and liquids*, Fifth Edition: McGRAW-HILL.

Rincon, Hernan, Shadley, John R., and Edmund F. Rybicki. "Erosion Corrosion Phenomena of 13Cr at Low Sand Rate Levels." Paper presented at the CORROSION 2005, Houston, Texas, April 2005.

Rowe, A. and Chou, J. 1970. Pressure-volume-temperature-concentration relation of aqueous sodium chloride solutions. *Journal of Chemical & Engineering Data* **15** (1): 61-66. https://doi.org/10.1021/je60044a016.

Sevindik, D., Erol, S., and Akin, S. 2024. Numerical modeling of the CO_2 injection in the Kızıldere geothermal field using multiple inter-well tracer tests. *Geothermics* **119**: 102964. https://doi.org/10.1016/j.geothermics.2024.102964.

Shock, E. and Koretsky, C. 1995. Metal-organic complexes in geochemical processes: Estimation of standard partial molal thermodynamic properties of aqueous complexes between metal cations and monovalent organic acid ligands at high pressures and temperatures. *Geochimica et Cosmochimica Acta* **59** (8): 1497-1532. https://doi.org/10.1016/0016-7037(95)00058-8.

Szizybalski, A., Zimmer, M., Pilz, P. et al. 2017. Results from twelve years of continuous monitoring of the soil CO_2 flux at the Ketzin CO_2 storage pilot site, Germany. *Energy Procedia* **125**: 543-548. https://doi.org/10.1016/j.egypro.2017.08.186.

Tokel, A. B., Akın, S., Akın, T. et al. 2023. Recent Soil Carbon Dioxide Flux Measurements at Kızıldere Geothermal Field. Presented at 48th Workshop on Geothermal Reservoir Engineering Stanford University, Stanford, California, February 6-8.

United States Environmental Protection Agency 2024. ADM Geologic Sequestration Well - Proposed Order SDWA-05-2025-0001, 9/19/24, https://www.epa.gov/il/adm-geologic-sequestration-well-proposed-order-sdwa-05-2025-0001.

United States Environmental Protection Agency 2024. Overview of Greenhouse Gases [Overviews and Factsheets], 9/19/24, https://www.epa.gov/ghgemissions/overview-greenhouse-gases accessed 25 December 2024.

Verdon, J., Kendall, J., White, D. et al. 2011. Linking microseismic event observations with geomechanical models to minimise the risks of storing CO_2 in geological formations. *Earth and Planetary Science Letters* **305**: 143-152. https://doi.org/10.1016/j.epsl.2011.02.048.

Wang, H., Precious Oyenowo, O., and Okuno, R. 2023. Aqueous formate solution for enhanced water imbibition in oil recovery and carbon storage in carbonate reservoirs. *Fuel* **345**: 128198. https://doi.org/10.1016/j.fuel.2023.128198.

Wang, H., Serra, V., and Okuno, R. 2025. Formate-enhanced CO_2 Mineralization with Carbonate, Mafic, And Ultramafic Rocks. SPE International Conference on Oilfield Chemistry. Galveston, Galveston, TX, USA, 9-10 April 2025.

Wolery, T.J. and Jarek, R.L. 2003. EQ3/6, Version 8.0 software's user manual. Software document no. 10813-UM-80-00, US DOE Office of Civilian Radioactive Waste Management, Office of Repository Development, Las Vegas, Nevada.

Xu, T., Zheng, L., and Tian, H. 2011. Reactive transport modeling for CO_2 geological sequestration. *Journal of Petroleum Science and Engineering* **78**: 765-777. https://doi.org/10.1016/j.petrol.2011.09.005.

Zhang, Z., Wang, T., Blunt, M. et al. 2020. Advances in carbon capture, utilization and storage. *Applied Energy* **278**: 115627. https://doi.org/10.1016/j.apenergy.2020.115627.